NF-κB protein expression associates with ^{18}F-FDG PET tumor uptake in non-small cell lung cancer: a radiogenomics validation study to understand tumor metabolism

Viswam S. Nair, MD MS[1], **Olivier Gevaert, PhD**[2], **Guido Davidzon, MD MS**[3], **Sylvia K. Plevritis, PhD**[2], and **Robert West, MD PhD**[4]

[1]Division of Pulmonary & Critical Care Medicine, 300 Pasteur Drive, Stanford University School of Medicine, Stanford CA, 94305

[2]Department of Radiology, 300 Pasteur Drive, Stanford University School of Medicine, Stanford CA, 94305

[3]Department of Radiology, Division of Nuclear Medicine, Loyola University Chicago Stritch School of Medicine, 2160 S. 1st Ave Maywood, IL 60153

[4]Department of Pathology, 300 Pasteur Drive, Stanford University School of Medicine, Stanford, CA 94305

Abstract

Introduction—We previously demonstrated that NF-κB may be associated with ^{18}F-FDG PET uptake and patient prognosis using radiogenomics in patients with non-small cell lung cancer (NSCLC). To validate these results, we assessed NF-κB protein expression in an extended cohort of NSCLC patients.

Methods—We examined NF-κBp65 by immunohistochemistry (IHC) using a Tissue Microarray. Staining intensity was assessed by qualitative ordinal scoring and compared to tumor FDG uptake (SUV_{max} and SUV_{mean}), Lactate Dehydrogenase A (LDHA) expression (as a positive control) and outcome using ANOVA, Kaplan Meier (KM), and Cox-proportional hazards (CPH) analysis.

Results—365 tumors from 355 patients with long-term follow-up were analyzed. The average age for patients was 67 ± 11 years, 46% were male and 67% were ever smokers. Stage I and II patients comprised 83% of the cohort and the majority had adenocarcinoma (73%). From 88 FDG PET scans available, average SUV_{max} and SUV_{mean} were 8.3 ± 6.6, and 3.7 ± 2.4 respectively. Increasing NF-κBp65 expression, but not LDHA expression, was associated with higher SUV_{max} and SUV_{mean} ($p = 0.03, 0.02$ respectively). Both NF-κBp65 and positive FDG uptake were significantly associated with more advanced stage, tumor histology and invasion. Higher NF-κBp65 expression was associated with death by KM analysis ($p = 0.06$) while LDHA was strongly associated with recurrence ($p = 0.04$). Increased levels of combined NF-κBp65 and LDHA expression were synergistic and associated with both recurrence ($p = 0.04$) and death ($p = 0.03$).

Corresponding Author. Viswam S. Nair MD MS, 300 Pasteur Drive, Grant Bldg, S021, Stanford University School of Medicine, Stanford, CA 94305, viswamnair@stanford.edu, Phone: 650-724-9635.

Publisher's Disclaimer: This is a PDF file of an unedited manuscript that has been accepted for publication. As a service to our customers we are providing this early version of the manuscript. The manuscript will undergo copyediting, typesetting, and review of the resulting proof before it is published in its final citable form. Please note that during the production process errors may be discovered which could affect the content, and all legal disclaimers that apply to the journal pertain.

Conflict of Interest: None of the authors have financial and personal relationships with other people or organizations that could inappropriately influence (bias) this work.

Conclusions—NF-κB IHC was a modest biomarker of prognosis that associated with tumor glucose metabolism on FDG PET when compared to existing molecular correlates like LDHA, which was synergistic with NF-κB for outcome. These findings recapitulate radiogenomics profiles previously reported by our group and provide a methodology for studying tumor biology using computational approaches.

Keywords

NSCLC; lung cancer; FDG PET; glucose metabolism; NFKB; RelA; LDH; radiogenomics

Introduction

Radiogenomics is an emerging field dedicated to discovering new associations amongst imaging and gene features that will improve our understanding of human disease and ultimately translate to improved patient care.[1] We have previously published a radiogenomics model of gene expression integrated with ^{18}F-2-deoxy-2-fluoro-*D*-glucose (FDG) PET imaging that suggests NF-κB (nuclear factor kappa-light-chain-enhancer of activated B cells) is a central node in tumor glucose metabolism and potentially related to patient prognosis.[2] In that study, we associated the gene expression of tumors for patients with non-small cell lung cancer (NSCLC) and FDG PET imaging data, and then examined the association of those FDG PET related genes and the imaging features themselves with outcome in separate cohorts. The result was a defined cluster of genes–or a metagene–of 508 individual genes that were associated with both FDG uptake and outcome. IPA network analysis (Ingenuity® Systems, Redwood City, CA) implicated NF-κB as a central node within this metagene and provided the rationale for us to proceed with further investigation since NF-κB is well established to play an important role in cancer development and FDG uptake is a surrogate for tumor glucose metabolism and may be prognostic clinically.[3]

NF-κB[4, 5] is an essential transcription factor that controls multiple cellular processes under normal and pathologic conditions, including tissue differentiation, inflammation, wound healing, angiogenesis and proliferation.[6] It is present in all tissues and most commonly is inactive in its cytosolic, bound form. Once released by inhibitor of nuclear factor kappa-B kinase (IκKB),[7] it then migrates to the nucleus to exert its influence on the cell.

Deranged NF-κB signaling is oncogenic for multiple reasons.[8] Mitogens like cigarette smoke activate NF-κB,[9] as do oncogenes like *myc*,[10] and *ras*.[11] Downstream signaling of NF-κB activation involves cell matrix remodeling,[12–14] cell adhesion,[15, 16] and chemotaxis,[17] all of which are important for angiogenesis and metastasis. This has led to interest in targeting NF-κB clinically[18] and to studies assessing patient prognosis with increased NF-κB expression in cancer.[19]

Major oncogenes or tumor suppressors like *myc*,[20] and *p53*[21–24] that regulate glucose metabolism, NF-κB,[10, 25] and in some cases both,[25, 26] have been reported. Exactly how NF-κB signaling interplays with the Warburg Effect[27, 28]–or aberrant tumor aerobic glycolysis–and tumor cell metabolism in general has not been well studied, particularly in the clinical setting.

Here, we follow-up on our initial radiogenomics work, where we observed a potential relationship between NF-κB and PET FDG uptake, by creating a large tissue microarray (TMA) to examine if NF-κB immunohistochemistry expression relates to tumoral FDG PET uptake and prognosis in patients with NSCLC.

Methods

Study cohort

Patient samples were retrieved from surgical pathology archives at the Stanford Medical Center's Department of Pathology and linked to a clinical database using the Cancer Center Database and STRIDE Database tools from Stanford.[29] We reviewed patients who had surgically treated disease and archival formalin-fixed, paraffin-embedded (FFPE) samples from 1995 through June 2010 for inclusion. Patients with samples of recurrent or metastatic disease only were excluded but treated samples (neo-adjuvant therapy) were allowed. Medical charts were reviewed to clinically annotate the tumor specimens with demographics, operative procedures, imaging data, and follow-up. Smoking history was defined as never, ever (quit more than one year ago or defined in the medical record as "former") and current (active smoking or quit one year ago or less) per the chart. Pathology reports were reviewed to confirm specimen pathology including stage, grade, histology and invasion status. For this study, tumor invasion was dichotomized as either (1) without any invasion be it pleural and/or lympho-vascular or (2) as any invasion be it pleural and/or lympho-vascular. All aspects of this study were IRB approved prior to its initiation in accordance with the Declaration of Helsinki guidelines for the ethical conduct of research. A waiver of informed consent was obtained for the subjects in this study according to Stanford's Institutional Review Board policy since this was a retrospective study of both alive and deceased patients, many of who were lost to follow-up.

Follow-up

Follow-up data was available for this cohort from 1995 through 2010. Recurrence was defined by either imaging or biopsy and those who did not have at least 6 months of follow-up were censored for further analyses. Area of recurrence was defined as within the lung (local metastasis), in the lymphatics or pleura (regional metastasis) or in distant organ sites like the liver, bone, or brain (distant metastasis). The National Death Index (NDI)[30] was used to define vital status through October 30, 2010. Patients not dead were assumed to be alive except for those who had left the country or were from other countries (who were censored) since the NDI relies on a social security number for vital status assessment. Synchronous tumors resected over time were eligible for prognostic assessment in patients with two primaries.

Tissue Microarray (TMA) Construction

The Stanford Lung Cancer TMA was developed from archival FFPE surgical specimens that contained viable tumor from duplicate slides that were reviewed by a board-certified pathologist (RW). The area of highest tumor content was marked manually for coring blocks corresponding to the slides. We then used single 0.6 mm cores to build the tissue microarray from this marked section. These cores were grouped by histology and stage and negative controls were taken from the West Lab that included a variety of benign and malignant tissues (65 cores) consisting of normal non-lung tissue (12 cores), abnormal non-lung tissue (13 cores), placental markers (23 cores) and normal lung (17 cores). Normal lung consisted of a specimen adjacent, but distinct, from tumor over the years 1995 through 2010 to assess the variability of staining by year. OligodT analysis was performed on the finished array to assess the architecture of selected cores and adequacy of tissue content prior to target IHC analysis. A co-registered Hematoxylin & Eosin slide was used as well to verify tumor location for cases where this was unclear on initial inspection. Since LDHA has been evaluated in NSCLC prognosis[31, 32] and potentially is also related to FDG uptake due to its involvement in cancer related glycolysis,[33, 34] we evaluated this target in addition to NF-κBp65.

Immunohistochemistry (IHC)

IHC was performed using standard methods.[35] In general, antibody titration optimization was performed starting with the manufacturer's recommendations followed by inspection of adequacy of staining on a separate cancer array with normal tissue controls. NF-κBp65 (Cell Signaling Technology, D14E12, XP™ Rabbit mAb, #8242) was incubated at a 1:800 dilution using citrate antigen retrieval for final expression analysis. LDHA (Santa Cruz Biotechnology, sc-137243, LDH-A (E-9) Ab) was incubated at 1:400 dilution using citrate antigen retrieval. For NF-κBp65 and LDHA, qualitative scoring was graded as negative (20% tumor cells stained), moderate (> 20% tumor cells stained) or high (75% tumor cells stained) intensity using standard bright-field microscopy at 20× to 40× magnification. Cores that had diffuse weak uptake throughout the tumor were graded as "moderate" and only those with intense staining in the majority of the tumor were assigned a "high" intensity score. We did not score non-tumor cells such as stroma or inflammatory cells and we only assessed cytoplasmic staining intensity for both antibodies. All cores were evaluated by VSN and arbitrated by RW. Missing cores, cores with less than 20 tumor cells, or staining artifacts were treated as non-scorable. Analyses were performed only after all core scoring had been finalized.

FDG-PET Imaging Data

FDG PET-CT images from 2003 through 2010 at Stanford University Medical Center that were most closely dated to the corresponding tumor pathology were retrieved to assess FDG uptake using a General Electric LS PET/CT with slice thickness 3 to 5 mm (GE, Milwaukee, WI, USA). Patients fasted for a minimum of six hours and a 370–550 mBq dose of FDG was administered. Fasting blood glucose was checked prior to FDG injection and patients were scanned approximately 60 minutes (range 45 to 65) after injection.

Only scans performed prior to resection or neo-adjuvant therapy were utilized leaving 88 in total after removing 2 with neo-adjuvant therapy administered prior to imaging. We extracted the maximum standard uptake value SUV_{max}, defined as the most intense voxel of uptake within a region of interest (ROI) circumscribing the tumor, and the mean standard uptake value SUV_{mean}, defined as the average voxel uptake across the same region of interest circumscribing the tumor, to assess FDG uptake within the primary tumor from which our TMA cores were sampled. The region of interest ranged from 1 cm to the entire cross-sectional area of the tumor. Patients who had synchronous tumors were eligible for analysis if each tumor had extractable FDG uptake information along with NF-κB expression data. We further dichotomized SUV_{max} at a positive value (>2.5)[36] for additional analysis.

Statistical Analysis

Cohort characteristics were tabulated using the mean and standard deviation for continuous variables or number with percent for categorical or ordinal variables. Differences between groups (i.e., for recurrence or vital status) were calculated using a Student's t-test or Wilcoxon test for continuous variables, and a Chi-squared or Fisher's exact test for categorical variables. Categorical levels of NF-κB staining were compared with continuous SUV_{max} using a Wilcoxon rank sum test. Categorical NF-κB expression and dichotomized SUV_{max} were compared to variables of interest using a Kruskal-Wallis, Chi-squared or Fisher's exact test. Kaplan-Meier (KM) curves were stratified by NF-κB, LDHA and combined NF-κB/LDHA expression scores for recurrence and death. Continuous SUV_{mean} and SUV_{max} values were associated with outcome along with other variables of interest using Cox proportional hazards (CPH) analysis for recurrence or death. All tests associations reported are for two-sided p-values and significance is defined as a p-value < 0.05. Calculations and figures were generated using SAS (v 9.3; Cary, NC).

Results

Seventy-two patients from our previous radiogenomics cohort were included in this TMA. The TMA was constructed from 369 cores from 359 patients, of which 4 were excluded since they were not primary lung tumors after detailed clinical review, leaving 365 cores for analysis (Table I). OligodT analysis showed 99% of the samples were of adequate quality. NF-κB staining was predominantly cytoplasmic and stained weakly or not at all on 147 cores, moderately on 151 cores and highly on 47 cores (Figure 1). Twenty NF-κBp65 cores were not interpretable due to artifact staining or tissue quality. LDHA cores stained strongly or moderately in 85 and 153 cores respectively and not at all in 114 cores (Supplement 2). Thirteen LDHA cores were not interpretable.

The average age for the cohort was 67 ± 11 years, and the majority of patients were stage I-II (83%), and Caucasian (62%) who smoked (67%) (Table I). Average tumor diameter was 3.5 ± 2.0 cm, and most were moderately to poorly differentiated (83%) adenocarcinoma (73%). During follow-up, 105 patients recurred (29%) and 170 died (47%). The most common recurrence sites were lung (50%), lymph node (22%), bone (19%) and brain (15%). Differences by group for recurrence were noted for adjuvant therapy, stage, SUV_{mean} and dichotomized SUV_{max}. For death, groups differed by age, ethnicity, stage and dichotomized SUV_{max}.

The mean SUV_{max} for available data was 8.3 ± 6.6 for 88 scans and 3.7 ± 2.4 for SUV_{mean}. SUV_{mean} and SUV_{max} varied by histology, with non-adenocarcinoma tumors having statistically higher uptake than adenocarcinoma tumors (p-value < 0.001 for both; Supplemental 1). Increasing SUV_{max} corresponded to higher NF-κB expression (6.3 ± 5.2, 9.0 ± 6.8, and 13.0 ± 8.7) for each expression level respectively; p-value $= 0.03$) and the same was true for SUV_{mean} (p-value $= 0.02$; Figure 2). LDHA expression, on the contrary, was not significantly different for dichotomized SUV_{max} or SUV_{mean} (Table II). When dichotomized at a threshold value of 2.5, higher SUV_{max} was associated with smoking status, stage, tumor size, grade, histology, and tumor invasion Comparatively, increasing NF-κB expression was significantly associated with stage, histology and tumor invasion (Table II). Similar to SUV_{max}, non-adenocarcinomas (squamous and other NSCLC histology) were associated with increased NF-κB expression when compared to adenocarcinomas (p-value $= 0.02$).

Outcome for this cohort of patients was as expected and in-line with reported literature estimates.[37] For example, increasing stage was associated with poorer outcome, five-year stage I survival was approximately 60%, and 64% of recurrences occurred within the first two years after resection (Supplement 3). As expected, well known prognostic variables like age, stage, tumor size, tumor invasion and tumor grade were significantly associated with recurrence or death (Table III).

Increasing FDG uptake levels were strongly associated with five-year recurrence by univariate CPH models and showed a trend with death (p-value $= 0.07$ and p-value $= 0.08$ for SUV_{max} and SUV_{mean} respectively) along with stage, tumor size, and tumor invasion (Table III). For increasing LDHA expression there was a trend towards, death and a significant association with recurrence (Table III, Figure 3). KM plots stratified by high or low NF-κB expression showed a strong trend with increasing level of expression for death (p-value $= 0.06$; Figure 3) that was synergistic with LDHA expression (high or low) (p-value $= 0.03$; Figure 3). NF-κB expression showed no trend for recurrence for any level but again was synergistic with LDHA expression (p-value $= 0.04$; Table III, Figure 3). We found no significant associations for NF-κB levels by local, regional, or distant metastatic sites.

Discussion

We show here that NF-κB IHC expression is related to tumor glucose metabolism as measured by FDG PET. Additionally, we show that both of these biomarkers are related to advancing stage, histology and tumor invasion–variables that have established prognostic implications.[37, 38] Our results support the recognized interplay of oncogenic, inflammatory and metabolic pathways in cancer by using a practical approach involving clinically relevant data. While previous studies have examined NF-κB expression and prognosis in other cancers [19] or in lung cancer as it relates to stage (which our study corroborates),[39] no previous study has examined NF-κB expression along with FDG uptake and prognosis using a large database of surgically treated NSCLC patients.

Our previous radiogenomics study[2] examined FDG PET imaging features in the context of metagene expression profiles and tissue IHC recapitulated this computational approach in a consistent manner with a stronger signal noted for glucose metabolism than smoking, which is a known pro-inflammatory state.[40] Namely, protein level expression representing a complementary level of molecular information was analyzed in an extended, larger cohort of patients using an *a priori* biologically driven hypothesis from gene network analysis. This illustrates the potential utility of the radiogenomics approach, provides new data on NF-κB in lung cancer, and warrants further investigation on how NF-κB expression is mechanistically linked with tumor glucose metabolism.

Recent findings in the literature are beginning to unravel the connections between oncogenesis, inflammation, and tumor bioenergetics. TP53 is both an indirect and direct regulator of glycolysis via TIGAR (TP53 inducible regulator of glycolysis and apoptosis) [41, 42] and G6PD,[21] and it has recently has been shown to regulate NF-κB via IκKB kinase. Additionally, NF-κB is activated downstream of excess lactate production, a hallmark of the Warburg Effect.[43] Interestingly, of several studies that have analyzed lung tumor IHC expression as it relates to FDG PET (including ki67, VEGF, EGFR, GLUT1, 3 and CAIX)[44–49] one study[50] confirmed that TP53 is related to both outcome and FDG uptake. TP53's control of GLUT1 and GLUT4[23] regulation supports this study's clinical observation since FDG is taken up primarily through GLUT1, and could explain the associations we found in our study as well.

Interestingly, LDHA tissue expression was associated with poorer outcome and did not associate with NF-κB expression or dichotomized FDG uptake but did show synergy with NF-κB for prognosis. LDHA and Lactate Dehydrogenase B (LDHB) are the primary subunits for LDH_{1-5}, whose subtype is defined by location. Subunits two thru five are composed primarily of LDHA, and LDH5 is well studied in the literature both at the tissue level and in circulation as a prognostic marker in lung cancer [31–34]. The lack of association with FDG uptake is surprising given LDHA's presumably stoichiometric relationship in glucose metabolism, however other pathways may be at play given the added value of LDHA in combination with NF-κB, and we have no precedent in the literature to compare our findings. We therefore encourage the readership to follow-up on our results.

Strengths of our study include the novelty and large TMA we were able to examine with long-term follow-up and annotation, yet there are several important limitations to consider. The NF-κB superfamily is composed of two protein classes [51] that exist either with a C-terminal ankyrin repeat motif (Class I, NF-κB) or trans-membrane activation domain (Class II, Rel; RelA = p65). However, we assessed cytosolic NF-κBp65 only since the antibody clone we used preferentially bound this complex (Figure 1). Because this is only one of the many protein complexes constituting "NF-κB," we did not fully delineate its biology by defining the active nuclear state.

We do not think the results in this paper are clinically actionable at this point. However, we do provide a proof-of-concept for validating radiogenomics studies for the clinical investigator in addition to adding to the extant literature on NF-κB tumor biology. Validation in other external cohorts would be a key to moving these findings further towards the clinical lab, as well as more standardized pathology analyses.[35] While developing imaging tracers or drugs to NF-κB would be hindered by the ubiquity of this pathway in humans, other targets that are intimately related to NF-κB tumor metabolism with specificity could be clinically relevant.

Lastly, we only had FDG PET data for a quarter of this cohort, so there could be undetected bias in patients who were differentially excluded based solely on the fact that they did not have FDG PET imaging. Since our measurement of FDG uptake depended on a two-dimensional cross-section of tumor that did not necessarily co-register with the single 0.6 mm tumor core taken from the TMA, there may have been an erosion of statistical signal in our analysis, particularly in light of tumor heterogeneity.

Conclusion

NF-κB protein expression and PET FDG uptake of primary tumors in NSCLC appear to be associated with each other as well as stage, histology and tumor invasion. Although NFKB was not associated with LDHA expression, these two markers were synergistic for prognosis. These results validate a previously reported, discovery-based exploration of radiogenomic profiles in NSCLC and add to the growing literature linking cell bioenergetics and inflammation in a clinically relevant model.

Supplementary Material

Refer to Web version on PubMed Central for supplementary material.

Acknowledgments

References

1. Rutman AM, Kuo MD. Radiogenomics: creating a link between molecular diagnostics and diagnostic imaging. Eur J Radiol. 2009; 70:232–241. [PubMed: 19303233]

2. Nair VS, Gevaert O, Davidzon G, Napel S, Graves EE, Hoang CD, et al. Prognostic PET 18F-FDG uptake imaging features are associated with major oncogenomic alterations in patients with resected non-small cell lung cancer. Cancer Res. 2012; 72:3725–3734. [PubMed: 22710433]

3. Berghmans T, Dusart M, Paesmans M, Hossein-Foucher C, Buvat I, Castaigne C, et al. Primary tumor standardized uptake value (SUVmax) measured on fluorodeoxyglucose positron emission tomography (FDG-PET) is of prognostic value for survival in non-small cell lung cancer (NSCLC): a systematic review and meta-analysis (MA) by the European Lung Cancer Working Party for the IASLC Lung Cancer Staging Project. J Thorac Oncol. 2008; 3:6–12. [PubMed: 18166834]

4. Sen R, Baltimore D. Inducibility of kappa immunoglobulin enhancer-binding protein Nfkappa B by a posttranslational mechanism. Cell. 1986; 47:921–928. [PubMed: 3096580]

5. Singh H, Sen R, Baltimore D, Sharp PA. A nuclear factor that binds to a conserved sequence motif in transcriptional control elements of immunoglobulin genes. Nature. 1986; 319:154–158. [PubMed: 3079885]

6. Aggarwal BB. Signalling pathways of the TNF superfamily: a double-edged sword. Nat Rev Immunol. 2003; 3:745–756. [PubMed: 12949498]

7. Hoffmann A, Levchenko A, Scott ML, Baltimore D. The IkappaB-NF-kappaB signaling module: temporal control and selective gene activation. Science. 2002; 298:1241–1245. [PubMed: 12424381]

8. Aggarwal BB. Nuclear factor-kappaB: the enemy within. Cancer Cell. 2004; 6:203–208. [PubMed: 15380510]

9. Anto RJ, Mukhopadhyay A, Shishodia S, Gairola CG, Aggarwal BB. Cigarette smoke condensate activates nuclear transcription factor-kappaB through phosphorylation and degradation of IkappaB(alpha): correlation with induction of cyclooxygenase-2. Carcinogenesis. 2002; 23:1511–1518. [PubMed: 12189195]

10. Klapproth K, Sander S, Marinkovic D, Baumann B, Wirth T. The IKK2/NF-{kappa}B pathway suppresses MYC-induced lymphomagenesis. Blood. 2009; 114:2448–2458. [PubMed: 19628709]

11. Dajee M, Lazarov M, Zhang JY, Cai T, Green CL, Russell AJ, et al. NF-kappaB blockade and oncogenic Ras trigger invasive human epidermal neoplasia. Nature. 2003; 421:639–643. [PubMed: 12571598]

12. Bond M, Fabunmi RP, Baker AH, Newby AC. Synergistic upregulation of metalloproteinase-9 by growth factors and inflammatory cytokines: an absolute requirement for transcription factor NF-kappa B. FEBS Lett. 1998; 435:29–34. [PubMed: 9755853]

13. Yan C, Wang H, Aggarwal B, Boyd DD. A novel homologous recombination system to study 92 kDa type IV collagenase transcription demonstrates that the NF-kappaB motif drives the transition from a repressed to an activated state of gene expression. FASEB J. 2004; 18:540–541. [PubMed: 14715692]

14. Tobar N, Villar V, Santibanez JF. ROS-NFkappaB mediates TGF-beta1-induced expression of urokinase-type plasminogen activator, matrix metalloproteinase-9 and cell invasion. Mol Cell Biochem. 2010; 340:195–202. [PubMed: 20204677]

15. Iademarco MF, McQuillan JJ, Rosen GD, Dean DC. Characterization of the promoter for vascular cell adhesion molecule-1 (VCAM-1). J Biol Chem. 1992; 267:16323–16329. [PubMed: 1379595]

16. Whelan J, Ghersa P, Hooft van Huijsduijnen R, Gray J, Chandra G, Talabot F, et al. An NF kappa B-like factor is essential but not sufficient for cytokine induction of endothelial leukocyte adhesion molecule 1 (ELAM-1) gene transcription. Nucleic Acids Res. 1991; 19:2645–2653. [PubMed: 1710341]

17. Ueda A, Ishigatsubo Y, Okubo T, Yoshimura T. Transcriptional regulation of the human monocyte chemoattractant protein-1 gene. Cooperation of two NF-kappaB sites and NF-kappaB/Rel subunit specificity. J Biol Chem. 1997; 272:31092–31099. [PubMed: 9388261]

18. Gilmore TD, Herscovitch M. Inhibitors of NF-kappaB signaling: 785 and counting. Oncogene. 2006; 25:6887–6899. [PubMed: 17072334]

19. Yu HG, Yu LL, Yang Y, Luo HS, Yu JP, Meier JJ, et al. Increased expression of RelA/nuclear factor-kappa B protein correlates with colorectal tumorigenesis. Oncology. 2003; 65:37–45. [PubMed: 12837981]

20. Dang CV. Rethinking the Warburg effect with Myc micromanaging glutamine metabolism. Cancer Res. 2010; 70:859–862. [PubMed: 20086171]

21. Jiang P, Du W, Wang X, Mancuso A, Gao X, Wu M, et al. p53 regulates biosynthesis through direct inactivation of glucose-6-phosphate dehydrogenase. Nat Cell Biol. 2011; 13:310–316. [PubMed: 21336310]

22. Mathupala SP, Heese C, Pedersen PL. Glucose catabolism in cancer cells. The type II hexokinase promoter contains functionally active response elements for the tumor suppressor p53. J Biol Chem. 1997; 272:22776–22780. [PubMed: 9278438]

23. Schwartzenberg-Bar-Yoseph F, Armoni M, Karnieli E. The tumor suppressor p53 down-regulates glucose transporters GLUT1 and GLUT4 gene expression. Cancer Res. 2004; 64:2627–2633. [PubMed: 15059920]

24. Zhang C, Lin M, Wu R, Wang X, Yang B, Levine AJ, et al. Parkin, a p53 target gene, mediates the role of p53 in glucose metabolism and the Warburg effect. Proc Natl Acad Sci U S A. 2011; 108:16259–16264. [PubMed: 21930938]

25. Royds JA, Dower SK, Qwarnstrom EE, Lewis CE. Response of tumour cells to hypoxia: role of p53 and NFkB. Mol Pathol. 1998; 51:55–61. [PubMed: 9713587]

26. Kawauchi K, Araki K, Tobiume K, Tanaka N. p53 regulates glucose metabolism through an IKK-NF-kappaB pathway and inhibits cell transformation. Nat Cell Biol. 2008; 10:611–618. [PubMed: 18391940]

27. Warburg O. On respiratory impairment in cancer cells. Science. 1956; 124:269–270. [PubMed: 13351639]

28. Warburg O. On the origin of cancer cells. Science. 1956; 123:309–314. [PubMed: 13298683]

29. Lowe HJFT, Hernandez PM, Weber SC. An Integrated Standards-Based Translational Research Informatics Platform. AMIA Annu Symp Proc. 2009:391–395. [PubMed: 20351886]

30. Cowper DC, Kubal JD, Maynard C, Hynes DM. A primer and comparative review of major US mortality databases. Ann Epidemiol. 2002; 12:462–468. [PubMed: 12377423]

31. Turna A, Solak O, Cetinkaya E, Kilicgun A, Metin M, Sayar A, et al. Lactate dehydrodgenase levels predict pulmonary morbidity after lung resection for non-small cell lung cancer. Eur J Cardiothorac Surg. 2004; 26:483–487. [PubMed: 15302039]

32. Danner BC, Didilis VN, Wiemeyer S, Stojanovic T, Kitz J, Emmert A, et al. Long-term survival is linked to serum LDH and partly to tumour LDH-5 in NSCLC. Anticancer Res. 2010; 30:1347–1351. [PubMed: 20530451]

33. Koukourakis MI, Giatromanolaki A, Sivridis E. Lactate dehydrogenase isoenzymes 1 and 5: differential expression by neoplastic and stromal cells in non-small cell lung cancer and other epithelial malignant tumors. Tumour Biol. 2003; 24:199–202. [PubMed: 14654714]

34. Kayser G, Kassem A, Sienel W, Schulte-Uentrop L, Mattern D, Aumann K, et al. Lactate-dehydrogenase 5 is overexpressed in non-small cell lung cancer and correlates with the expression of the transketolase-like protein 1. Diagn Pathol. 2010; 5:22. [PubMed: 20385008]

35. Beck AH, Espinosa I, Gilks CB, van de Rijn M, West RB. The fibromatosis signature defines a robust stromal response in breast carcinoma. Lab Invest. 2008; 88:591–601. [PubMed: 18414401]

36. Fletcher JW, Kymes SM, Gould M, Alazraki N, Coleman RE, Lowe VJ, et al. A comparison of the diagnostic accuracy of 18F-FDG PET and CT in the characterization of solitary pulmonary nodules. J Nucl Med. 2008; 49:179–185. [PubMed: 18199626]

37. Rami-Porta R, Crowley JJ, Goldstraw P. The revised TNM staging system for lung cancer. Ann Thorac Cardiovasc Surg. 2009; 15:4–9. [PubMed: 19262443]

38. Maeda R, Yoshida J, Ishii G, Hishida T, Nishimura M, Nagai K. Risk factors for tumor recurrence in patients with early-stage (stage I and II) non-small cell lung cancer: patient selection criteria for adjuvant chemotherapy according to the seventh edition TNM classification. Chest. 2011; 140:1494–1502. [PubMed: 21622548]

39. Tang X, Liu D, Shishodia S, Ozburn N, Behrens C, Lee JJ, et al. Nuclear factorkappaB (NF-kappaB) is frequently expressed in lung cancer and preneoplastic lesions. Cancer. 2006; 107:2637–2646. [PubMed: 17078054]

40. Yang SR, Chida AS, Bauter MR, Shafiq N, Seweryniak K, Maggirwar SB, et al. Cigarette smoke induces proinflammatory cytokine release by activation of NF-kappaB and posttranslational modifications of histone deacetylase in macrophages. Am J Physiol Lung Cell Mol Physiol. 2006; 291:L46–L57. [PubMed: 16473865]

41. Li H, Jogl G. Structural and biochemical studies of TIGAR (TP53-induced glycolysis and apoptosis regulator). J Biol Chem. 2009; 284:1748–1754. [PubMed: 19015259]

42. Bensaad K, Tsuruta A, Selak MA, Vidal MN, Nakano K, Bartrons R, et al. TIGAR, a p53-inducible regulator of glycolysis and apoptosis. Cell. 2006; 126:107–120. [PubMed: 16839880]

43. Hirschhaeuser F, Sattler UG, Mueller-Klieser W. Lactate: a metabolic key player in cancer. Cancer Res. 2011; 71:6921–6925. [PubMed: 22084445]

44. Yamamoto Y, Nishiyama Y, Ishikawa S, Nakano J, Chang SS, Bandoh S, et al. Correlation of 18F-FLT and 18F-FDG uptake on PET with Ki-67 immunohistochemistry in non-small cell lung cancer. Eur J Nucl Med Mol Imaging. 2007; 34:1610–1616. [PubMed: 17530250]

45. Usuda K, Sagawa M, Aikawa H, Ueno M, Tanaka M, Machida Y, et al. Correlation between glucose transporter-1 expression and 18F-fluoro-2-deoxyglucose uptake on positron emission tomography in lung cancer. Gen Thorac Cardiovasc Surg. 2010; 58:405–410. [PubMed: 20703861]

46. Vesselle H, Schmidt RA, Pugsley JM, Li M, Kohlmyer SG, Vallires E, et al. Lung cancer proliferation correlates with [F-18] fluorodeoxyglucose uptake by positron emission tomography. Clin Cancer Res. 2000; 6:3837–3844. [PubMed: 11051227]

47. Marom EM, Aloia TA, Moore MB, Hara M, Herndon JE 2nd, Harpole DH Jr, et al. Correlation of FDG-PET imaging with Glut-1 and Glut-3 expression in early-stage non-small cell lung cancer. Lung Cancer. 2001; 33:99–107. [PubMed: 11551404]

48. Zhang L, Higashi K, Ishigaki Y, Ueda Y, Sakuma T, Takegami T, et al. Assessment of VEGF-D expression measured by immunohistochemical staining and F-18 FDG uptake on PET as biological prognostic factors for recurrence in patients with surgically resected lung adenocarcinoma. Ann Nucl Med. 2010; 24:533–540. [PubMed: 20607627]

49. Dooms C, van Baardwijk A, Verbeken E, van Suylen RJ, Stroobants S, De Ruysscher D, et al. Association between 18F-fluoro-2-deoxy-D-glucose uptake values and tumor vitality: prognostic value of positron emission tomography in early-stage non-small cell lung cancer. J Thorac Oncol. 2009; 4:822–828. [PubMed: 19487964]

50. Taylor MD, Smith PW, Brix WK, Wick MR, Theodosakis N, Swenson BR, et al. Fluorodeoxyglucose positron emission tomography and tumor marker expression in non-small cell lung cancer. J Thorac Cardiovasc Surg. 2009; 137:43–48. [PubMed: 19154901]

51. Gilmore TD. Introduction to NF-kappaB: players, pathways, perspectives. Oncogene. 2006; 25:6680–6684. [PubMed: 17072321]
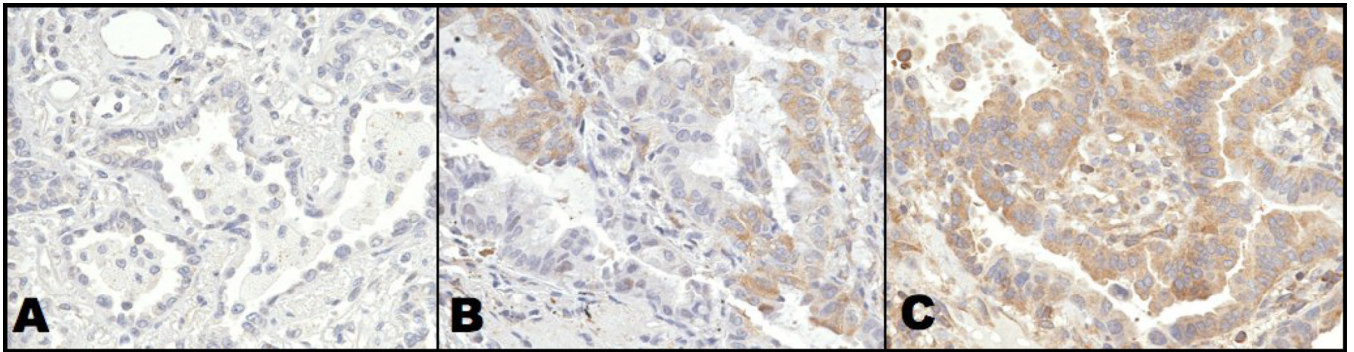
Figure 1.
Representative 0.6 mm cores of NSCLC from a tissue microarray that included 369 NSCLC samples along with a variety of benign and malignant tissues (65 samples) are shown at 40× magnification for A) low B) moderate and C) high intensity staining (see methods for definition). As shown, the antibody selected for this study stained primarily tumor cytoplasm (brown) compared with nuclei (blue) that did not stain.
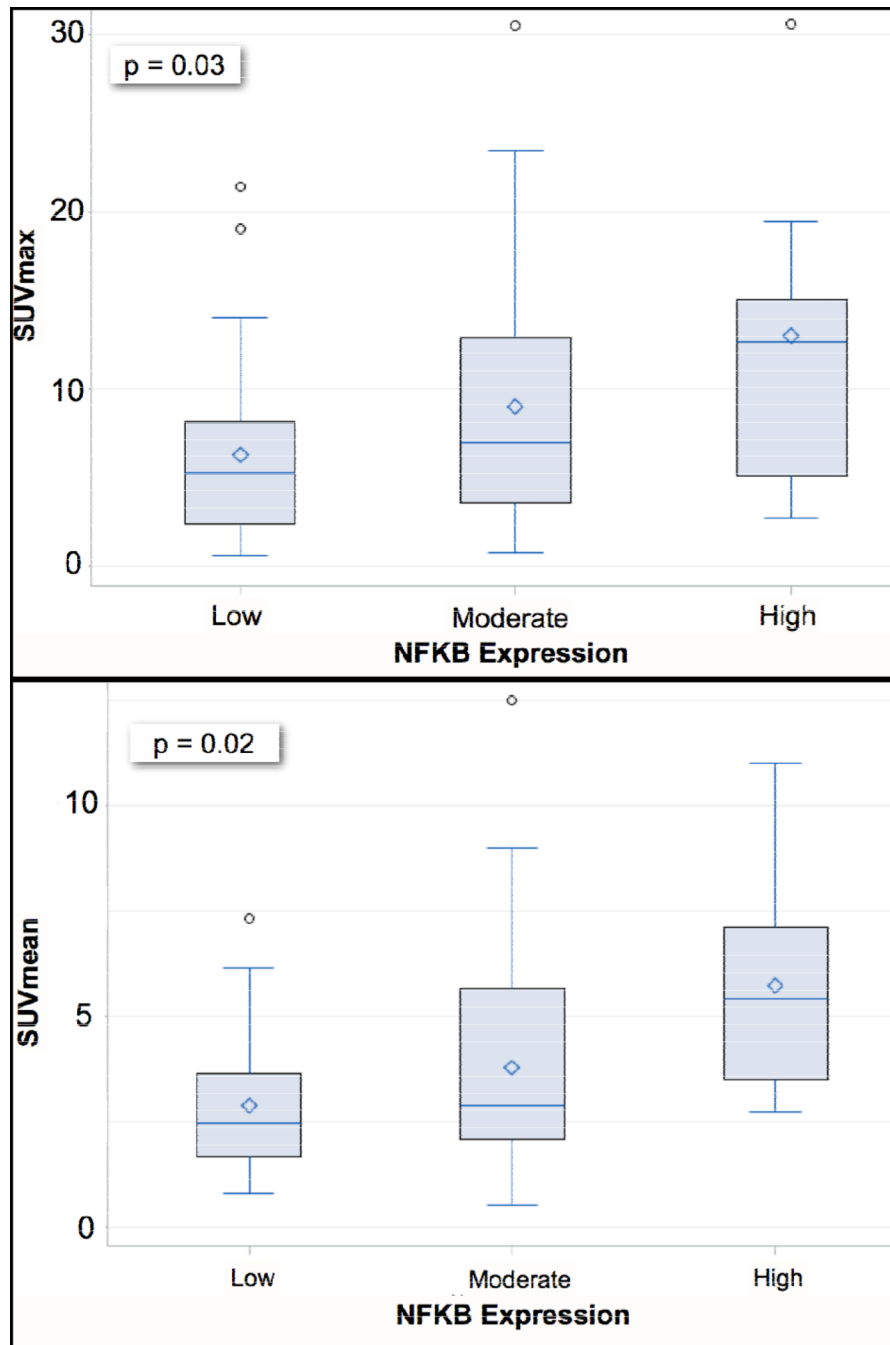
Figure 2.
Boxplots of FDG uptake metrics as continuous variables are shown for increasing NF-κB expression levels. There was a significant difference between groups for both (A) SUV_{max} and (B) SUV_{mean}. The y-axis represents SUV level and the x-axis NF-κB expression level by group.
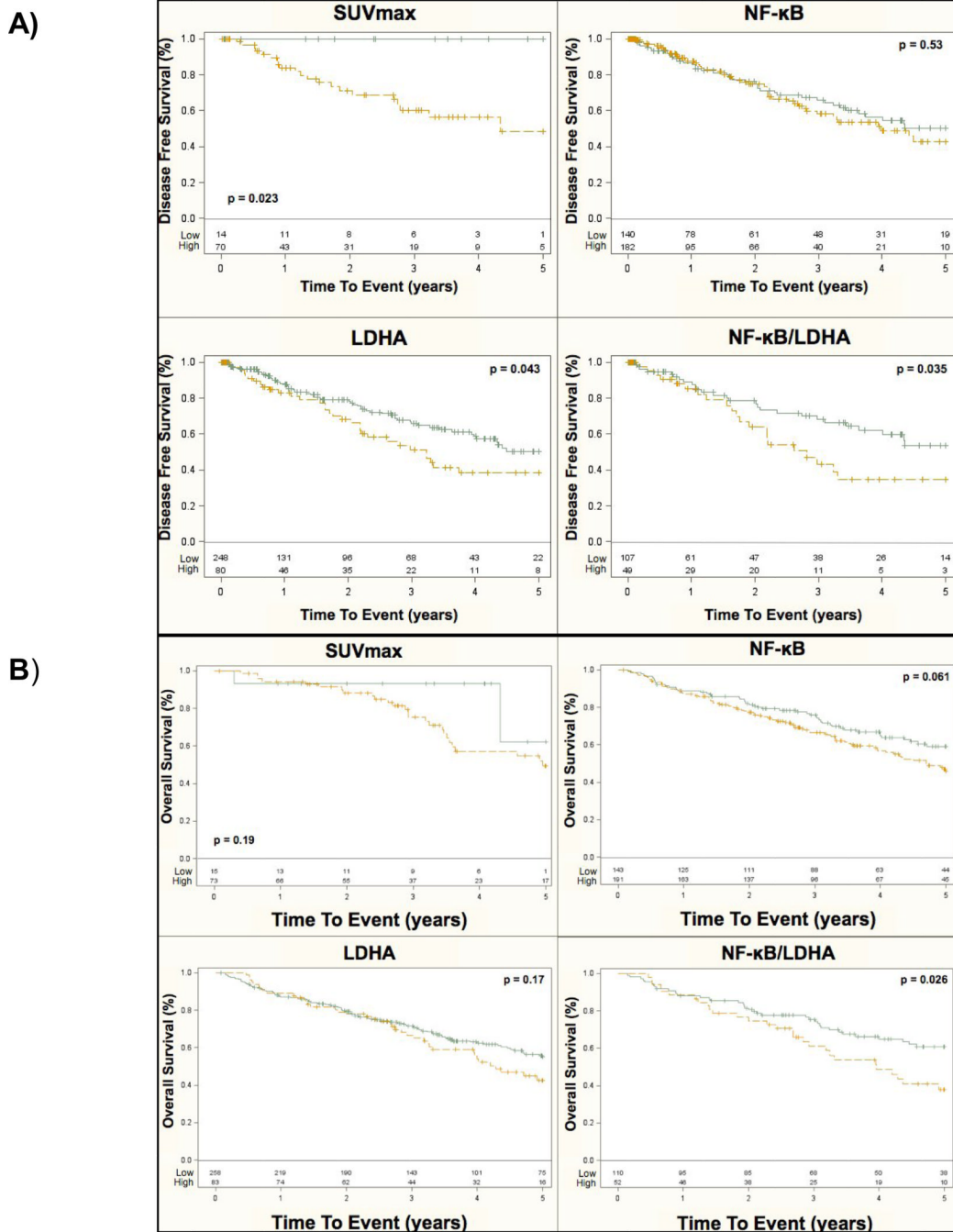
Figure 3.
Kaplan–Meier curves are shown by stage for (A) five-year disease free survival and (B) overall survival for SUV_{max}, NF-κB, LDHA and NF-κB/LDHA combined expression. The probability of event is on the y-axis and time-to-event is on the x-axis. The number of events is listed at the bottom of each graph and the p-value for significance between groups is shown within each figure. IHC expression levels were combined as high (moderate or high expression levels, yellow line) vs. low (green line) for simplicity of interpretation.

Table I

Cohort Characteristics

Variable*	All (n=365)	No Recur (n=239)[†]	Recur (n=105)	Alive (n=195)	Death (n=170)
Age (years)	67.2 (11.0)	67.4 (10.5)	67.4 (10.5)	66.0 (10.6)	68.8 (11.4)[§]
Gender (% male)	167 (46)	102 (43)	50 (48)	80 (40)	86 (51)
Race					
Caucasian	226 (62)	150 (63)	60 (25)	107 (55)	119 (70)[§]
Asian	58 (16)	33 (14)	22 (9)	39 (20)	19 (11)
Black	11 (3)	14 (6)	9 (4)	8 (4)	3 (2)
Other	70 (19)	42 (18)	13 (5)	41 (21)	29 (17)
Smoking Status[‡]					
Never	78 (21)	44 (18)	28 (27)	52 (27)	26 (15)
Ever	169 (46)	113 (47)	48(46)	90 (46)	79 (46)
Current	78 (21)	82 (34)	18 (17)	36 (18)	42 (25)
Unknown	40 (11)	26 (11)	11 (10)	17 (9)	23 (14)
Additional Therapy					
Neo-adjuvant	27 (7)	14 (6)	11 (10)[§]	12 (6)	15 (9)
Adjuvant	68 (19)	28 (12)	38 (36)	30 (15)	38 (5)
Neither/unknown	270 (74)	197 (82)	56 (53)	153 (78)	117 (7)
Tumor diameter (cm)	3.5 (2.0)	3.3 (1.9)	3.7 (2.8)	2.9 (1.5)	4.1 (2.2)
Stage (AJCC 7th ed.)					
I–II	304 (83)	211 (88)	81 (77)[§]	179 (92)	125 (74)[§]
III–IV	61 (17)	28 (12)	24 (23)	16 (8)	45 (26)
Histology					
Adenocarcinoma	265 (73)	172 (72)	79 (75)	142 (73)	123 (72)
Squamous	68 (19)	47 (20)	15 (14)	37 (19)	31 (18)
Other NSCLC	33 (9)	20 (8)	11 (11)	16 (8)	16 (9)
Grade (n = 343)					
Low	59 (17)	44 (18)	14 (13)	39 (20)	20 (12)

Variable*	All (n=365)	No Recur (n=239)[†]	Recur (n=105)	Alive (n=195)	Death (n=170)
Moderate	177 (52)	68 (28)	53 (50)	51 (26)	84 (49)
High	107 (31)	115 (48)	31 (30)	93 (48)	56 (34)
Time to PET (days)[¶]	51 (88)	54 (114)	46 (36)	47 (105)	52 (47)
SUV_{max} (n = 88)	8.3 (6.6)	7.6 (6.3)	10.2 (8.2)	7.4 (6.3)	9.8 (7.0)
SUV_{mean} (n = 69)	3.7 (2.4)	6.5 (6.5)	11.3 (9.0)[§]	3.4 (2.4)	4.3 (2.4)
SUV_{max} (>2.5)	16/94 (17)	50/65 (77)	22/22 (100)[§]	44/58 (76)	34/36 (94)[§]
NF-κB expression					
Low	147 (40)	95 (40)	46 (44)	80 (41)	77 (45)
Moderate	151 (41)	101 (42)	38 (36)	74 (38)	67 (39)
High	47 (13)	31 (13)	14 (13)	28 (14)	19 (11)
Not Interpretable	20 (5)	12 (5)	7 (7)	13 (7)	7 (4)
LDHA expression					
Low	114	76 (32)	33 (31)	61 (31)	53 (31)
Moderate	153	108 (45)	34 (32)	83 (43)	70 (41)
High	85	45 (19)	35 (33)	41 (21)	44 (26)
Not Interpretable	13	10 (4)	3 (3)	10 (5)	3 (2)

AJCC = American Joint Committee on Cancer.

*
Standard deviation and percent shown for continuous or categorical variables respectively.

[†]Excluding post-operative deaths and advanced disease at diagnosis.

[‡]See methods for category definitions.

[¶]From PET scan to operation.

[§]Differences by p-value < 0.05.

Table II

NF-κB and SUV$_{max}$ Associations

	n	NF-κB[†] p-value	n	SUV$_{max}$[‡] p-value
Age (years)	345	0.40	88	0.34
Ethnicity[*]	339	0.97	87	0.28
Sex[*]	339	0.13	88	0.79
Smoking Status[*]	307	0.79	**86**	**0.006**
N stage (AJCC VII)	343	0.06	88	0.06
TNM Stage (AJCC VII)[*]	**339**	**0.02**	**88**	**0.02**
Tumor Size (cm)	342	0.19	**88**	**0.03**
Tumor Grade[*]	317	0.35	**84**	**0.002**
Histology[*]	**339**	**0.02**	**88**	**0.046**
Tumor Invasion	**332**	**0.01**	**85**	**0.04**
LDHA[†]	341	0.26	89	0.40

Associations are shown in bold when significant and shaded when both biomarkers were significant. n = number assessed for calculation.

[*] See Table 1 for method of categorizing analytic variables on left.

[†] IHC for NF-κB and LDHA expression stratified by high (moderate & high IHC staining combined) or low expression.

[‡] Threshold of 2.5 for SUV$_{max}$.

Table III

Univariate Cox Proportional Hazards Models

Variable	Recurrence			Death		
	p-value	HR	CI	p-value	HR	CI
Age (years)	**0.02**	**1.02**	**1.00–1.04**	0.19	0.99	0.97–1.00
Sex (male)	0.32	1.18	0.85–1.62	0.35	1.22	0.81–1.82
Ethnicity[†]	0.61	0.97	0.87–1.09	0.69	1.03	0.89–1.19
Smoking Status[†]	0.87	0.98	0.71–1.33	0.11	1.22	0.95–1.58
TNM Stage *[†]	**<.0001**	**2.65**	**2.05–3.43**	**<.0001**	**1.94**	**1.60–2.34**
T classification (1–4) *	**<.0001**	**1.96**	**1.52–2.54**	**<.0001**	**1.81**	**1.50–2.19**
N classification (1–3) *	**<.0001**	**2.36**	**1.81–3.07**	**<.0001**	**1.97**	**1.61–2.41**
Tumor size (cm)	**<.0001**	**1.29**	**1.16–1.43**	**<.0001**	**1.26**	**1.18–1.36**
Histology[†]	0.97	1.01	0.73–1.38	0.96	1.01	0.79–1.28
Tumor invasion[†]	**<.0001**	**2.33**	**1.53–3.56**	**<.0001**	**2.16**	**1.56–3.00**
Grade[†]	**0.03**	**1.31**	**1.03–1.67**	0.20	1.23	0.90–1.68
SUV$_{max}$	**0.002**	**1.10**	**1.04–1.17**	0.07	1.04	1.00–1.09
SUV$_{mean}$	**0.0005**	**1.39**	**1.16–1.68**	0.08	1.13	0.99–1.30
NF-κB (Low vs. High)[†‡]	0.46	1.17	0.77–1.79	0.06	1.39	0.99–1.94
LDHA (Low vs. High)[†‡]	**0.04**	**1.58**	**1.02–2.43**	0.15	1.30	0.91–1.85
NF-κB/LDHA (Low vs. High)[§]	**0.04**	**1.84**	**1.03–3.27**	**0.03**	**1.73**	**1.06–2.82**

Significant values are in bold. HR = Hazard ratio. CI = 95% confidence interval.

*
According to AJCC VII.

[†]
See Table 1 for levels.

[‡]
Moderate and high expression levels were combined for the low vs. high binary comparison for both NF-κB and LDHA.

[§]
Defined as high expression levels for both markers (n=66) vs. low expression levels for both markers (n=162).